Heterochrony underpins natural variation in *Cardamine hirsuta* leaf form

Maria Cartolano[a], Bjorn Pieper[a], Janne Lempe[a], Alex Tattersall[b], Peter Huijser[a], Achim Tresch[c,d], Peter R. Darrah[b], Angela Hay[a], and Miltos Tsiantis[a,1]

[a]Department of Comparative Development and Genetics, Max Planck Institute for Plant Breeding Research, 50829 Cologne, Germany; [b]Department of Plant Sciences, University of Oxford, Oxford OX1 3RB, United Kingdom; [c]Botanical Institute, University of Cologne, 50647 Cologne, Germany; and [d]Max Planck Institute for Plant Breeding Research, 50829 Cologne, Germany

Edited by Caroline Dean, John Innes Centre, Norwich, United Kingdom, and approved July 10, 2015 (received for review October 17, 2014)

A key problem in biology is whether the same processes underlie morphological variation between and within species. Here, by using plant leaves as an example, we show that the causes of diversity at these two evolutionary scales can be divergent. Some species like the model plant *Arabidopsis thaliana* have simple leaves, whereas others like the *A. thaliana* relative *Cardamine hirsuta* bear complex leaves comprising leaflets. Previous work has shown that these interspecific differences result mostly from variation in local tissue growth and patterning. Now, by cloning and characterizing a quantitative trait locus (QTL) for *C. hirsuta* leaf shape, we find that a different process, age-dependent progression of leaf form, underlies variation in this trait within species. This QTL effect is caused by *cis*-regulatory variation in the floral repressor *ChFLC*, such that genotypes with low-expressing *ChFLC* alleles show both early flowering and accelerated age-dependent changes in leaf form, including faster leaflet production. We provide evidence that this mechanism coordinates leaf development with reproductive timing and may help to optimize resource allocation to the next generation.

Cardamine hirsuta | natural variation | compound leaf | heterochrony | Flowering Locus C

Leaves of seed plants present an attractive model to address the genetic basis for morphological diversity at different scales because they show considerable variation between and within species, and their morphology also differs according to developmental age in a phenomenon known as heteroblasty (1) (Fig. 1). Leaves can be classified into two broad morphological classes: simple, where the blade is entire, or dissected (also referred to as compound), where the blade comprises individual leaflets (Fig. 1*A*). Both simple and dissected leaves emerge from a pluripotent structure called the shoot apical meristem. Previous work has identified two processes that underlie such interspecies diversification of leaf shape. The first is the generation of lateral cell proliferation axes that give rise to leaflets. This process typically involves reactivation of meristem genes in leaves such as class I Knotted1-like homeobox (*KNOX1*) and CUP-SHAPED COTYLEDON (*CUC*) genes, which influence the patterning of peaks of auxin activity that are required for leaflet formation (2–6). The second is the action of local growth repressors at the flanks of emerging leaflet primordia that promote leaflet separation. This process involves the leaf-specific homeobox gene REDUCED COMPLEXITY (*RCO*) (7). Furthermore, in dissected leafed species, leaf complexity is regulated by the activity of TEOSINTE BRANCHED1/CYCLOIDEA/PROLIFERATING CELL FACTOR (*TCP*) genes, which modulate the competence of the leaf margin to respond to organogenic signals (8, 9).

Results and Discussion

Despite progress in understanding the genetic pathways controlling leaflet development and leaf shape diversity between species (10, 11), their contribution to intraspecific differences in leaf morphology remains unclear. To study this problem, we exploited natural variation in leaf form of *Cardamine hirsuta* (Fig. 1*B*), which shows marked age-dependent variation (12) (Fig. 1*C* and Fig. S1 *A* and *B*). We performed quantitative trait locus (QTL) analysis in an F8 recombinant inbred line (RIL) mapping population descended from a cross between the Oxford (Ox) and Washington (Wa) strains (13) for the following traits: leaflet number; leaflet shape, quantified by extended eigenshape analysis (14); and leaf size (Fig. 2*A*, Fig. S1 *C–M*, and Table S1). Notably, no QTL for the analyzed leaf traits mapped to loci known or thought to underlie interspecific differences in leaf shape between simple and dissected leafed species, such as the *KNOX1* genes SHOOT MERISTEMLESS (*STM*) and BREVIPEDICELLUS (*BP*) (6, 15), *RCO* (7, 16), *TCP4* (8, 9), *CUC3*, or the microRNA *MIR164A* and its targets *CUC1–2* (5, 17, 18) (Fig. 2*A*). Therefore, the genetic basis for diversity in leaf form between and within species may be distinct in this instance.

In the RIL population, phenotypic variation for leaf size, complexity, and leaflet shape correlated with flowering time, suggesting that these traits may be under common genetic control (Fig. S1*N*). Consistent with this result, we found that a single QTL on linkage group 6 (QTL-LG6) explained most of the phenotypic variation for leaflet number on leaf 5, as well as cumulatively over the first seven leaf nodes; leaflet shape; leaflet area; and also flowering time (Fig. 2*A*, Fig. S1 *C–M*, and Table S1). The direction of the allelic effects of this QTL on leaflet number were opposite from the difference between the founding strains because the Wa strain showed more leaflets than Ox (Fig. S1 *A* and *B*), whereas

Significance

A key problem in biology is whether the same processes underlie morphological variation between and within species. Here, we show that the causes of leaf shape diversity at these two evolutionary scales can be divergent. Some species have simple leaves, whereas others bear complex leaves comprising leaflets. Previous work indicated that these interspecific differences result mostly from variation in local tissue growth and patterning. Now we find that a different process, age-dependent shape progression, underlies within-species variation in complex leaf morphology. Specifically, in plants with accelerated aging and early flowering, leaves progress to adult shapes with more leaflets, faster than their slower-aging counterparts. This mechanism coordinates leaf development with reproductive timing and may influence resource allocation to seeds.

Author contributions: M.C. and M.T. designed research; M.C., B.P., J.L., A. Tattersall, P.H., and A.H. performed research; P.R.D. contributed new analytic tools; M.C., B.P., J.L., A. Tattersall, P.H., A. Tresch, P.R.D., A.H., and M.T. analyzed data; M.C. and M.T. wrote the paper with input from B.P., J.L., and A.H; M.T. directed the study.

The authors declare no conflict of interest.

This article is a PNAS Direct Submission.

Freely available online through the PNAS open access option.

Data deposition: The sequences reported in this paper have been deposited in the GenBank database (accession nos. KM110949 and KM096577–KM096584).

[1]To whom correspondence should be addressed. Email: tsiantis@mpipz.mpg.de.

This article contains supporting information online at www.pnas.org/lookup/suppl/doi:10.1073/pnas.1419791112/-/DCSupplemental.

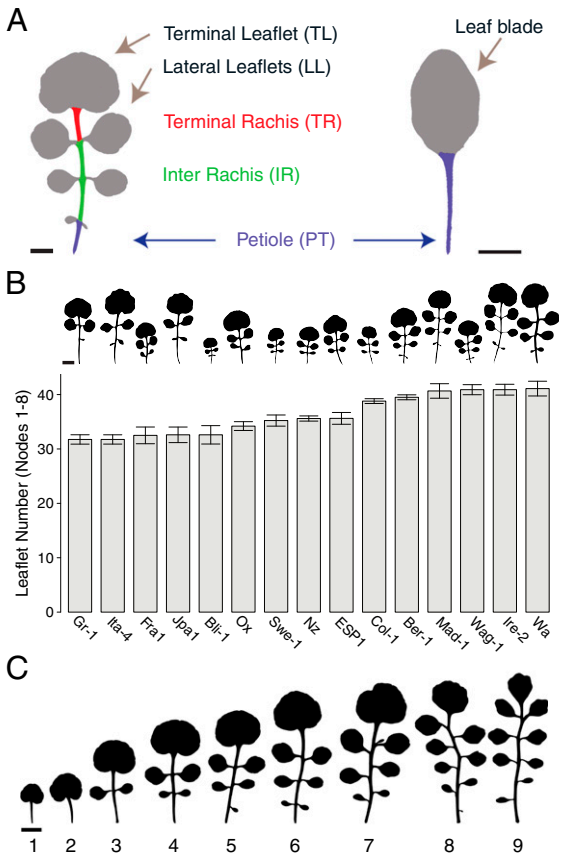

Fig. 1. Morphological diversity of leaves across different scales. (*A*) Morphology of *C. hirsuta* (Ox) and *A. thaliana* (Col-0) rosette leaves; different parts of the leaf are indicated. (*B*, *Upper*) Silhouettes of the fifth rosette leaf illustrate diversity in leaf morphology of natural *C. hirsuta* strains. (*B*, *Lower*) Quantification of total leaflet number in the first eight rosette leaves is shown in the bar chart. Data are reported as means ± SD. (*C*) Silhouettes of the first nine rosette leaves from a typical heteroblastic series in *C. hirsuta* (Ox).

the Wa allele at QTL-LG6 reduced leaflet number. This allelic behavior is consistent with a genetic architecture of multiple loci with both negative and positive effects (19). We validated QTL-LG6 for the number of leaflets produced on the fifth rosette leaf and flowering time using heterogeneous inbred families (HIFs) (20, 21) and fine-mapped it to a 13-kb interval on chromosome 6 (Fig. 2 *B–D*), which contains five ORFs, including the *C. hirsuta* ortholog of FLOWERING LOCUS C (*ChFLC*) (Fig. S2*A*). *FLC* is a well-studied MCM1/AGAMOUS/DEFICIENS/SRF (*MADS*) box gene that represses flowering (22–24). We found that *ChFLC* expression was reduced in the HIF homozygous for the Ox allele (HIF_{Ox}), compared with those carrying the Wa allele (HIF_{Wa}) (Fig. S2*B*), suggesting that natural allelic variation at *ChFLC* underlies QTL-LG6 and pleiotropically influences leaf form and flowering time. For complementation analysis, we transformed HIF_{Ox} with the genomic $ChFLC_{Wa}$ allele and found that the introduction of the transgene decreased leaflet number and increased flowering time in the direction predicted by the QTL analysis (Fig. 2 *A* and *E–L*). Similar allelic effects for flowering time were observed when we complemented the *Arabidopsis thaliana flc-3* mutant [*FRI-Sf2; flc*-3 (24, 25)] with $ChFLC_{Wa}$ and $ChFLC_{Ox}$ alleles, confirming that $ChFLC_{Ox}$ is a weaker allele compared with $ChFLC_{Wa}$ (Fig. S2*C*). Because the amino acid sequences of both alleles are identical but their expression levels differed, we concluded that regulatory changes at *ChFLC* underlie the QTL-LG6 effect (Fig. S2*D*). Consistent with this view, analysis of transgenic *FRI-Sf2 flc*-3 plants harboring chimeric constructs between the *ChFLC* Wa and Ox alleles indicated that the delayed flowering conferred by the Wa allele is attributable to the first intron (Fig. 2*M*), which was previously shown to influence the expression of natural *FLC* alleles in *A. thaliana* (26–32). Only three SNPs in this intron differentiate the Ox from the Wa allele, making them strong candidates for contributing to QTL-LG6, one of which, SNP203, lies in the conserved nucleation region (Fig. S2 *E* and *F* and Table S2). In conclusion, natural allelic variation in the floral repressor *ChFLC* influences leaf morphology. Specifically, reduced expression of *ChFLC* results in both early flowering and increased leaflet number at leaf 5 and cumulatively over the first seven leaf nodes.

To understand how *ChFLC* influences leaf development, we focused on heterochrony (33, 34). *FLC* influences developmental timing in *A. thaliana* (35, 36); therefore, we hypothesized that its effect on leaf form in *C. hirsuta* might be heterochronic, such that *ChFLC* influences age-related changes in leaf development. *C. hirsuta* heteroblasty is characterized by pronounced but gradual age-dependent changes in leaflet number, area, and shape (Figs. 1*C* and 3 *A* and *B*; Fig. S3 *A–E*). The allelic state of *ChFLC* influenced this progression as follows: Leaflet number increased more rapidly after leaf 4 along the heteroblastic progression in early flowering HIF_{Ox} and reached the maximum leaflet number at an earlier node than HIF_{Wa} plants, with the maximum leaflet number being identical for both genotypes (Fig. 3*C* and Fig. S3*F*). Moreover, the shape of the terminal leaflet in early flowering HIF_{Ox} progressed more rapidly from a kidney-shaped to a wedge-shaped morphology, compared with late-flowering HIF_{Wa} (Fig. 3*D* and Fig. S3*F*). These results indicate that *ChFLC* affects leaf form by influencing the rate of age-dependent progression of development. The shape of the last rosette leaf before flowering (LLBF) differed between *ChFLC* genotypes, such that HIF_{Ox} had a more wedge-shaped terminal leaflet and higher perimeter-to-surface ratio for the whole leaf than HIF_{Wa} (Fig. S3 *G* and *H*). Leaf geometry also differed between *ChFLC* genotypes at other leaf nodes, which can be seen by comparing leaflet number between HIF_{Ox} and HIF_{Wa} leaves with equivalent terminal leaflet shapes (Fig. 3*E*). Specifically, we identified five nodes in HIF_{Wa} plants, where an identical terminal leaflet shape did not correspond to an identical leaflet number at any node in HIF_{Ox}; two nodes in HIF_{Wa} plants had terminal leaflet shapes unique to this *ChFLC* genotype and not observed in HIF_{Ox} (Fig. 3*E*). Finally, distinct combinations of leaflet number and terminal leaflet shape were specific to each *ChFLC* allele, such that each trait was a significant and independent predictor of *ChFLC* genotype in the HIFs ($P < 0.05$; Wald test; Fig. S3*I*). This finding highlights how distinct dissected leaf forms can be attained by combining separate contributing features—e.g., leaflet shape and number—which themselves show different rates of age-dependent variation (Fig. 3 *C* and *D*). These shape differences are not indirect effects of differences in the timing of leaf initiation, because initiation rate does not differ between the two *ChFLC* genotypes before flowering (Fig. 3*F*). In conclusion, the allelic state of *ChFLC* affects leaf morphology in three ways. First, leaflet shape and number progress to adult trait values more rapidly, and cumulative leaflet number over seven nodes is higher in plants carrying the Ox allele compared with the Wa allele. Second, the form of the LLBF differs between the two genotypes. Finally, different combinations of distinct age-dependent shape elements create distinct adult leaf geometries.

To understand how the allelic status of *ChFLC* influences heteroblasty, we studied phase transitions. Vegetative shoot development progresses from a juvenile to an adult vegetative phase, and the transition is closely related to the competence to respond to flower-inducing signals (37, 38). The timing of this transition and the relative length of the juvenile and adult vegetative phases

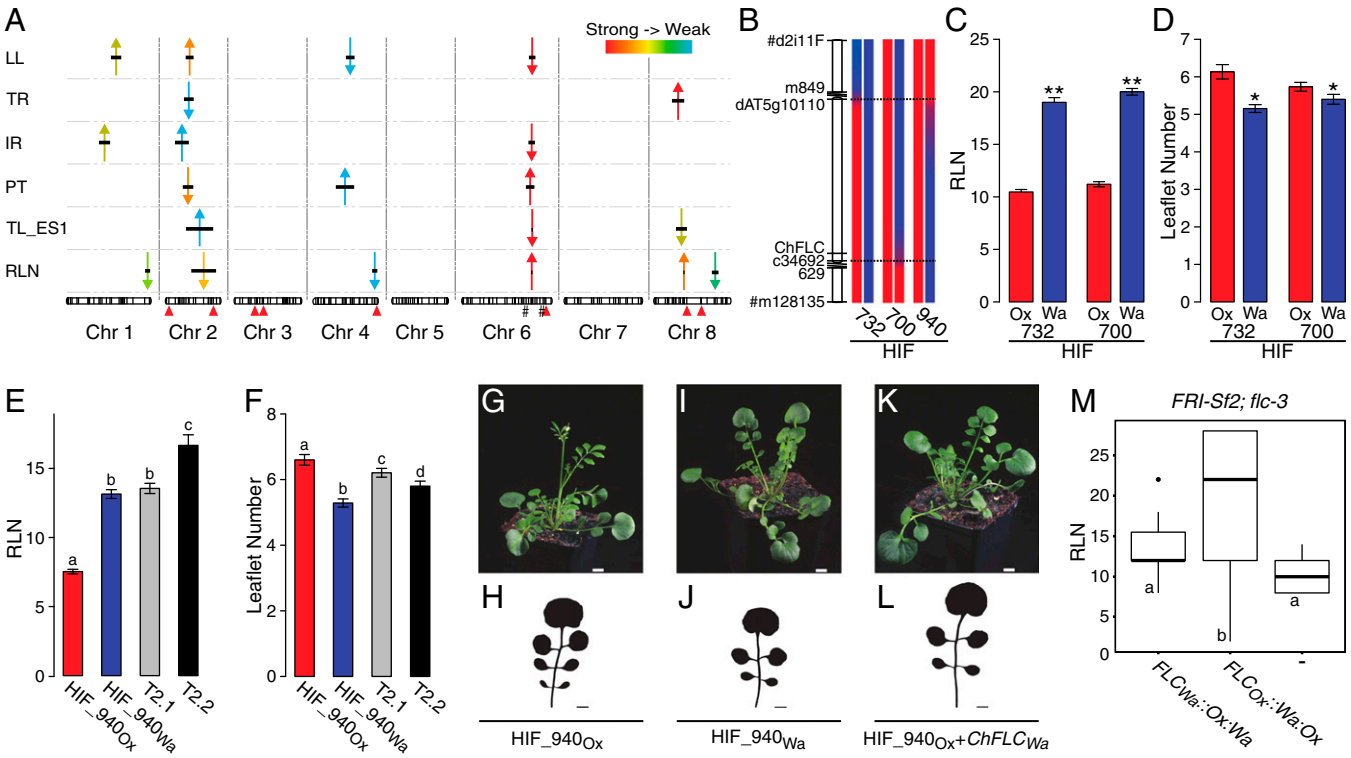

Fig. 2. Natural variation in the regulatory sequences of *ChFLC* underlies phenotypic diversity in leaf morphology and flowering time in *C. hirsuta*. (*A*) Schematic representation of QTL mapped in Ox × Wa RILs using composite interval mapping for six traits. Shown from top to bottom are leaflet number (LL), terminal rachis length (TR), inter rachis length (IR), petiole length (PT), terminal leaflet shape (TL-ES1), and rosette leaf number (RLN). Leaf traits were quantified on the fifth rosette leaf. Horizontal black lines indicate the 1.5 logarithm of odds support interval for QTL. The magnitude of QTL effects is indicated by a color gradient ranging from red (strong effect) to light blue (weak effect). Arrowheads indicate the direction of the QTL effect by pointing either upward or downward according to whether the Wa allele at the QTL increases or decreases the trait value when substituted for the Ox allele. Red arrowheads below the chromosomes indicate the position of characterized leaf patterning genes. From left to right, these are: *STM*, *CUC3*, *CUC1*, *TCP4*, *MIR164A*, *RCO*, *BP*, and *CUC2*. Hashtags on chromosome 6 indicate markers used to validate QTL-LG6. (*B*) Schematic diagram of QTL fine mapping using HIFs. Genetic markers are shown on the left, and Ox (red) and Wa (blue) genotypes are indicated on chromosomes of three different HIFs. Black dotted lines mark the boundaries of the fine mapped region. (*C* and *D*) Validation of *ChFLC* allelic effects using HIFs; the Ox allele (red) reduces RLN (*C*) and increases leaflet number (*D*) compared with the Wa allele (blue) ($n = 15$). $^{*}P < 0.05$; $^{**}P < 0.01$ (Student's *t* test). (*E* and *F*) Transgenic complementation of HIF940 carrying the $ChFLC_{Ox}$ allele ($HIF940_{Ox}$; red bar) with the $ChFLC_{Wa}$ genomic locus (two independent transgenic lines shown; gray and black bars). (*E*) RLN is fully complemented to $HIF940_{Wa}$ value (blue bar) in T2.1 (gray bar) and further increased in T2.2 (black bar). (*F*) Leaflet number is partially complemented to $HIF940_{Wa}$ value (blue bar) in T2.1 (gray bar) and T2.2 (black bar). Significant differences between genotypes determined by ANOVA and post hoc Tukey's test are indicated by letters; $P < 0.05$ ($n = 15$ per genotype). Leaflet number was quantified in rosette leaf five. Data are reported as means ± SD. (*G–L*) Photographs of plants (*G*, *I*, and *K*) and silhouettes of rosette leaf five (*H*, *J*, and *L*) of transgenic lines and HIFs described in *E* and *F*. (*M*) Boxplot of RLN in *A. thaliana FRI-Sf2;flc*-3 untransformed (–) or transformed with constructs containing the *ChFLC* genomic locus from Wa and Ox where the first intron is exchanged (FLC_{Wa}::*Ox:Wa* and FLC_{Ox}::*Wa:Ox*). Significant differences between genotypes determined by ANOVA and post hoc Tukey's test are indicated by letters; $P < 0.01$ ($n = 30$ per genotype). (Scale bars: 1 cm.)

often influence age-dependent changes in leaf form (39). On this basis, we investigated whether *ChFLC* affects leaf shape by modulating the timing of the juvenile-to-adult phase change in *C. hirsuta*. The first leaf that produces abaxial trichomes marks the time point of the juvenile-to-adult transition in *A. thaliana* (40). *C. hirsuta* leaves lack abaxial trichomes, and we could not identify another obvious morphological feature that discretely marks this transition (Fig. S3 *A–E* and *J*). Therefore, we identified the time point of the juvenile-to-adult phase change in *C. hirsuta* near isogenic lines (NILs) at the *ChFLC* locus by performing a photoperiod-shift experiment, where we used failure to respond to photoperiodic floral induction to identify juvenile plants (*SI Materials and Methods*) (38). By these criteria, we placed the end of juvenility between 5 and 7 DAS, when both genotypes responded to the photoperiodic induction of flowering (Fig. 3*G*). At this stage, both genotypes had produced on average three leaves at the shoot apical meristem (Fig. 3*F* and Fig. S3*K*). Therefore, allelic variation at *ChFLC* does not affect the onset of the juvenile-to-adult transition but, rather, influences the rate at which adult features are acquired. Growth analysis of developing leaves revealed that leaves of the early flowering NIL_Ox expanded faster and produced more leaflets per unit leaf length than NIL_Wa (Fig. 3 *H* and *I* and Fig. S3*L*). These observations indicate an acceleration of the leaf development program, including leaflet initiation, in the early flowering genotypes. From these results, we conclude that natural variation in a heterochronic pathway, which affects the length of the adult vegetative phase, influences heteroblastic progression in *C. hirsuta* by modulating the rate at which leaves mature and produce leaflets. Although *FLC* affects heteroblasty in *A. thaliana* (36), quantitative shape comparisons show that the consequences of heterochronic variation on leaf geometry are more pronounced in the complex leaf of *C. hirsuta* (Fig. S4*A*).

Next, we tested whether accelerated acquisition of adult leaf morphology in early flowering genotypes reflected a developmental feedback of the flowering state to developing vegetative leaves. We hypothesized that such a feedback might exist because accelerated flowering in response to inductive photoperiod also increased the rate of heteroblastic progression, in a manner reminiscent of the early flowering $ChFLC_{Ox}$ allele (Fig. S4*B*). We

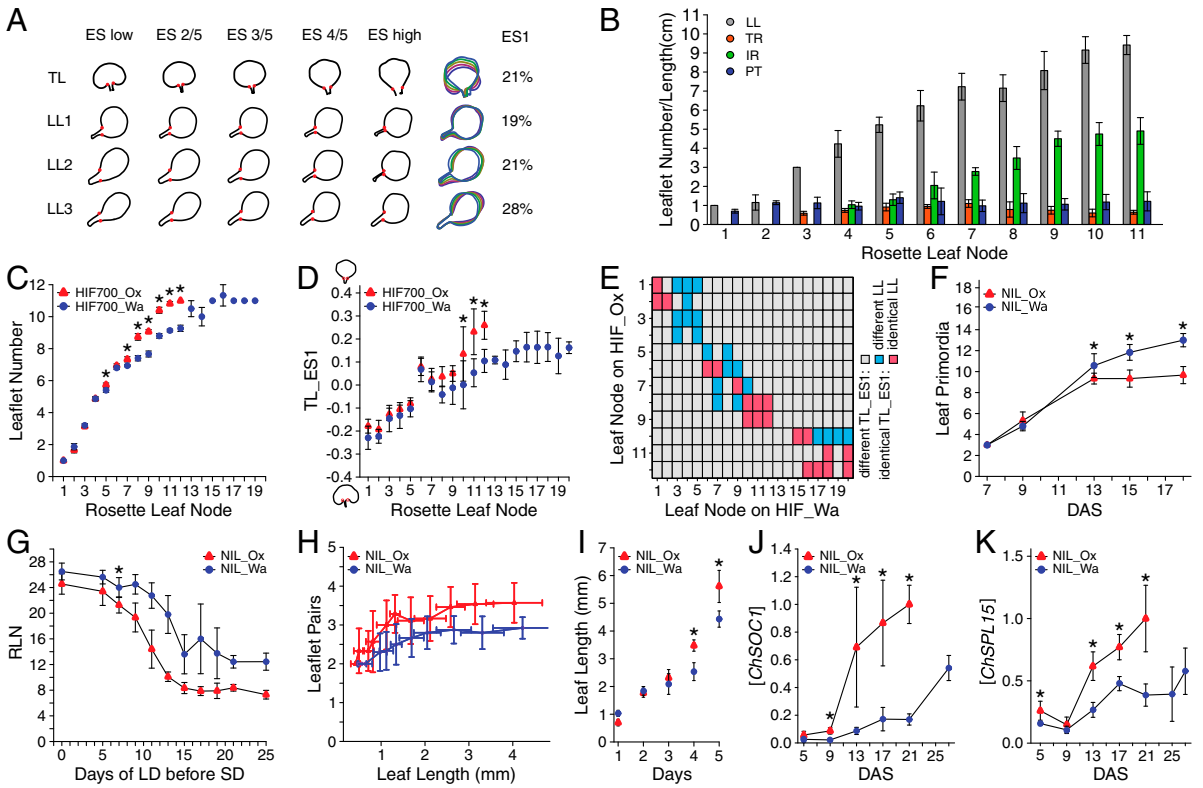

Fig. 3. Heterochronic variation caused by allelic diversity at *ChFLC* underlies natural variation in *C. hirsuta* leaf morphology. (*A* and *B*) *C. hirsuta* heteroblasty is characterized by continuous changes in leaf shape and size. (*A*) Extended eigenshape analysis was performed on the terminal leaflet (TL) and first (LL1), second (LL2), and third (LL3) pairs of lateral leaflets along the heteroblastic series of Ox. Models describing shape variation along the first eigenshape axis (ES1) and the variance explained by ES1 are shown. (*B*) Quantification of leaflet number (LL), terminal rachis (TR), inter rachis (IR), and petiole (PT) length in successive rosette leaves of Ox. (*C* and *D*) Leaflet number (*C*) and terminal leaflet shape (TL-ES1; *D*) in successive rosette leaves of HIF700 segregating for *ChFLC* [$n = 15$ per genotype (*C*); $n = 5$ per genotype (*D*)]. (*E*) Comparison of leaflet number between nodes of HIF_{Ox} and HIF_{Wa} with identical terminal leaflet shape (TL_ES1). Pairs of nodes with different TL_ES1 are shown in gray, and those with identical TL_ES1 in either blue or red depending on whether the leaflet number differed significantly between these nodes or not, respectively. Results were obtained by analyzing HIF732 and HIF700 jointly. (*F*) Leaf primordia visible at the shoot apical meristem plotted against DAS ($n = 15$ per genotype). No significant differences in leaf initiation rate are observed before 13 DAS when *ChFLCOx* has flowered. (*G*) Photoperiod sensing shift experiment: rosette leaf number (RLN) of NILs plotted against the number of LD experienced before transfer to SD. Asterisk indicates the point on the *x* axis when both genotypes showed a significant response to floral induction ($P < 0.05$ by Student's *t* test). (*H*) Average number of leaflet pairs of NILs plotted against a moving average of leaf length. (*I*) Length of the ninth rosette leaf measured for five consecutive days during early ontogenesis (*G* and *H*; $n = 15$ per genotype). (*J* and *K*) Expression levels of *ChSOC1* (*J*) and *ChSPL15* (*K*), measured by quantitative RT-PCR (qRT-PCR), increase significantly faster in NIL_Ox than NIL_Wa during development. Mean values and SDs are shown. *$P < 0.01$ (Student's *t* test).

observed that the *ChFLC* allelic status still affected leaflet number and flowering time, even when plants were grown under short-day conditions that delay flowering in *C. hirsuta*. However, in this case, the effect was shifted to later leaves in the heteroblastic series (Fig. S4 *C* and *D*). That the effect of *ChFLC* on leaf complexity cannot be uncoupled from flowering, even in noninductive conditions, suggests that *ChFLC* influences leaf shape, concomitant with its effect on the floral transition. Consistent with this view, we first detected differences in the expression of the floral integrators and likely targets of *FLC*, ChFLOWERING LOCUS T (*FT*) and ChSUPPRESSOR OF OVEREXPRESSION OF CO 1 (*ChSOC1*) (41, 42), between NIL_Ox and NIL_Wa at 9 days after sowing (DAS) (Fig. 3*J* and Fig. S4*G*). At this stage, long-day-grown plants have initiated four or five leaves (Fig. 3*F* and Fig. S3*K*), which is coincident with the first phenotypic differences in the heteroblastic progression between the two genotypes (Fig. 3*C* and Fig. S4 *E* and *F*). ChSQUAMOSA PROMOTER BINDING PROTEIN-LIKE 15 (*ChSPL15*) is another potential target of *ChFLC* (35), for which transcript levels rise faster in NIL_Ox than in NIL_Wa (Fig. 3*K* and Fig. S4 *H*–*K*). *SPL15* contributes to both flowering- and vegetative-phase transitions in *A. thaliana* (38, 43), which makes *ChSPL15* a strong candidate for mediating the effects of *ChFLC* on *C. hirsuta* leaf shape.

We have shown that *ChFLC* influences heteroblasty by regulating the adult vegetative phase, such that early flowering plants produce more complex adult leaf shapes at an earlier leaf node than their late-flowering counterparts (Fig. 4*A*). We reasoned that if this coordination between heteroblasty and reproductive timing is physiologically relevant, then genotypes lacking it should show perturbations in aspects of development that are influenced by it. Because flowering time has been suggested to influence seed yield (44, 45), we hypothesized that coordination of leaf growth with flowering may be part of a reproductive strategy to optimize resource allocation for the next generation. To test this idea, we evaluated the consequence of disrupting the coordination between leaf heteroblasty and flowering time on seed weight, by studying exceptional RIL families where this correlation is not found. To identify these lines, we first grouped RILs depending on their *ChFLC* allele, and then compared seed weight of lines belonging to the extreme tails of the distribution in leaflet number in each group (Fig. S5 *A* and *B*). Mean seed weight was significantly lower in early flowering $ChFLC_{Ox}$ RILs that had low leaflet number compared with the $ChFLC_{Ox}$ RILs with high leaflet number (Fig. 4*B* and Fig. S5 *C* and *D*). We did not detect any significant effect of flowering time on seed weight (ANOVA: RLN, $P = 0.67$; RLN × Leaflet, $P = 0.54$), which

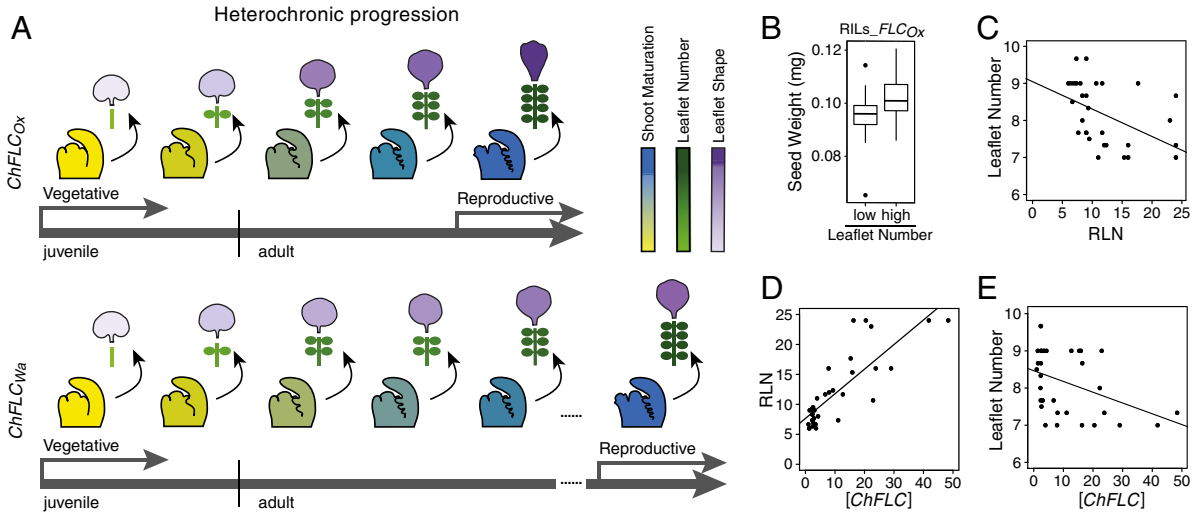

Fig. 4. The impact of *ChFLC* on heteroblasty, the correlation with seed weight, and the prevalence of *ChFLC*-dependent leaflet number variation in *C. hirsuta*. (*A*) Cartoon summarizing how *ChFLC*-dependent shoot maturation influences heteroblasty in *C. hirsuta*. The weaker $ChFLC_{Ox}$ allele causes increased leaflet number and rapid terminal leaflet shape changes at equivalent nodes compared with the stronger $ChFLC_{Wa}$ allele, owing to faster progression through the adult vegetative phase of the shoot. Differential age-dependent variation of leaflet number and terminal leaflet shape results in adult leaves with divergent morphologies. In addition, the weaker allele results in earlier flowering. Gray arrows mark the juvenile, adult vegetative, and reproductive phases. Meristems with developing leaves are colored following a gradient from yellow (not competent to flower) to dark blue (flowering), which reflects shoot maturation. Schematic representations of heteroblastic leaf traits are colored following a gradient from low leaflet number and juvenile leaflet shape (light green and purple, respectively) to high leaflet number and adult leaflet shape (dark green and purple, respectively). Leaf primordia and lateral and terminal leaflets are not drawn to scale. (*B*) Boxplot showing the median and interquartile range of seed weight of RILs selected for their leaflet number and for having the Ox allele at the *ChFLC* locus. Mean seed weight of low leaflet number (5–5.6) and high leaflet number (6–8) RILs is significantly different ($P < 0.05$ by ANOVA). (*C*) Differences in RLN (*x* axis) can explain variation in leaflet number (*y* axis) in a sample of 33 *C. hirsuta* strains ($R^2 = 0.25$; $P < 0.03$). (*D* and *E*) Variation in *ChFLC* expression measured by qRT-PCR (*x* axis) can explain differences in RLN (*D*; *y* axis; $R^2 = 0.68$; $P < 0.001$; $n = 35$) and leaflet number on leaf 7 (*E*; *y* axis; $R^2 = 0.15$; $P < 0.01$; $n = 33$). Transcript abundance is shown relative to that of the Ber-1 strain, which had the lowest *ChFLC* expression levels in our sample.

excludes the possibility that residual genetic variation for flowering time segregating in the RILs underlies differences in seed weight between RILs with low and high leaflet number. Thus, early flowering $ChFLC_{Ox}$ RIL plants that failed to acquire high leaflet number showed reduced seed weight. A plausible interpretation of these results is that early flowering plants optimize their leaf growth program to support seed set in the context of a shorter life cycle. One possibility is that leaves with increased adult character and more leaflets have a higher capacity to produce and/or transfer photosynthetic metabolites to floral tissues (46).

By investigating leaf shape in additional *C. hirsuta* accessions, we showed that the contribution of *ChFLC* to *C. hirsuta* leaflet number diversity is broadly informative for diversification patterns within the species, and not confined to the Ox and Wa genotypes. A major QTL controlling both flowering time and leaflet number was detected at the *ChFLC* locus in a different Ox × Gr-1 RIL population derived from a Greek founder strain (Fig. S5 *E*, *F*, and *I*). Additionally, both flowering time and leaflet number cosegregated with markers linked to the *ChFLC* locus in an Ox × Jpa1 HIF derived from a founder strain from Japan (Fig. S5 *G*–*I*). Finally, in a panel of 33 natural strains, 25% of the variation in leaflet number could be explained by flowering-time variance (Fig. 4*C*), whereas *ChFLC* expression levels explained 15% of the variation in leaflet number and 68% of the variation in flowering time (Fig. 4 *D* and *E*). From these results, we conclude that allelic diversity at *ChFLC* is a key contributor to natural variation in *C. hirsuta* leaf form. Natural variation in the *FLC* gene has been widely described to contribute to differences in flowering time within the Brassicaceae (23, 47–50). Given that *FLC* also acts as an environmental sensor (30, 51), it is possible that evolutionary changes in its regulation provide an opportunity for concerted modulation of leaf growth with flowering time in response to changing environments, making this gene a "hot spot" for evolutionary diversification. This view is also consistent with the hypothesis that regulatory divergence in pleiotropic genes provides a favorable path for morphological evolution to occur (52, 53).

Our work identifies heterochronic variation arising through regulatory evolution as a key driver of leaf shape diversity at the intraspecific scale, whereas developmental pathways controlling tissue patterning and local growth appear to dominate at the scale of interspecific variation in crucifers (5–7, 34). Flowering time can diversify rapidly in annuals such as *C. hirsuta*, so this coordinated regulation of leaf shape and flowering time by *ChFLC* may provide a mechanism for trait integration that anchors vegetative growth to reproduction to optimize resource allocation to seeds (48). Similar examples were reported as early as 1944 in cotton (54, 55), where early flowering genotypes developed leaves with increased complexity, and our work provides a framework to interpret these results from diverse taxa. However, heteroblasty can be uncoupled from reproduction in other examples (56), and early flowering can be associated with decreased, rather that increased, leaf complexity (57). Therefore, the timekeeping activity of common genetic modules may tend to associate flowering time with the rate of progression of vegetative development, but whether and how this tendency is expressed in different species may depend on the interplay of these timekeeping modules with lineage-specific leaf developmental programs, ecological challenges, reproductive strategies, and drift.

Materials and Methods

Plants were grown in controlled environment chambers under long-day (16h/8h; day/night) or short-day (8h/16h; day/night) conditions. All *C. hirsuta* strains used in this work are listed in Table S3 and the Ox x Wa F8 RIL population was previously described (13). Variation in shape of the terminal leaflet was quantified by Extended Eigenshape analysis (14). For the photoperiod-shift sensing experiment, plants were grown in LD conditions and transferred to SD

conditions 0–25 days after sowing. Detailed methods for plant growth conditions, phenotyping, QTL and statistical analysis, morphometric analysis, transgenic plant construction, quantitative RT-PCR, DNA sequencing, and microscopy can be found in the *SI Materials and Methods* and Tables S4 and S5.

ACKNOWLEDGMENTS. We thank S. Poethig and C. Alonso-Blanco for helpful discussions; G. Coupland for critical reading of the manuscript; M. Rast, J. Lamb, A. Hallab, X. Gan, E. Kirdök, J. Pietsch, S. Höhmann, B. Grosardt, I. Will, R. Pabst, N. MacLeod, and J. D. Krieger for assistance in molecular biology, phenotypic characterization, and bioinformatics; and M. Koornneef for donating *C. hirsuta* strains. This work was supported by Deutsche Forschungsgemeinschaft Priority Programme "Adaptomics" Grant TS 229/1-1 (to M.T. and A.H.); Biotechnology and Biological Sciences Research Council Grants BB/H011455/1 (to M.T.), BB/H006974/1 (to M.T. and A.H.); the Gatsby Charitable Foundation (M.T.); Cluster of Excellence on Plant Science (M.T.); HFSP-RGP0047/2010 (M.T.); the Minerva Programme of the Max Planck Society (A.H.) and a Max Planck Society core grant (M.T.). M.C. was supported by a Federation of European Biochemical Societies postdoctoral fellowship.

1. Goebel K (1900) *Organography of Plants Especially of the Archegoniatae and Spermatophyta* (Clarendon, Oxford).
2. Barkoulas M, Hay A, Kougioumoutzi E, Tsiantis M (2008) A developmental framework for dissected leaf formation in the Arabidopsis relative *Cardamine hirsuta*. *Nat Genet* 40(9):1136–1141.
3. Bharathan G, et al. (2002) Homologies in leaf form inferred from *KNOXI* gene expression during development. *Science* 296(5574):1858–1860.
4. Bilsborough GD, et al. (2011) Model for the regulation of *Arabidopsis thaliana* leaf margin development. *Proc Natl Acad Sci USA* 108(8):3424–3429.
5. Blein T, et al. (2008) A conserved molecular framework for compound leaf development. *Science* 322(5909):1835–1839.
6. Hay A, Tsiantis M (2006) The genetic basis for differences in leaf form between *Arabidopsis thaliana* and its wild relative *Cardamine hirsuta*. *Nat Genet* 38(8): 942–947.
7. Vlad D, et al. (2014) Leaf shape evolution through duplication, regulatory diversification, and loss of a homeobox gene. *Science* 343(6172):780–783.
8. Ori N, et al. (2007) Regulation of *LANCEOLATE* by *miR319* is required for compound-leaf development in tomato. *Nat Genet* 39(6):787–791.
9. Shleizer-Burko S, Burko Y, Ben-Herzel O, Ori N (2011) Dynamic growth program regulated by LANCEOLATE enables flexible leaf patterning. *Development* 138(4): 695–704.
10. Chitwood DH, et al. (2014) Resolving distinct genetic regulators of tomato leaf shape within a heteroblastic and ontogenetic context. *Plant Cell* 26(9):3616–3629.
11. Efroni I, Eshed Y, Lifschitz E (2010) Morphogenesis of simple and compound leaves: A critical review. *Plant Cell* 22(4):1019–1032.
12. Rubio-Somoza I, et al. (2014) Temporal control of leaf complexity by miRNA-regulated licensing of protein complexes. *Curr Biol* 24(22):2714–2719.
13. Hay AS, et al. (2014) *Cardamine hirsuta*: A versatile genetic system for comparative studies. *Plant J* 78(1):1–15.
14. MacLeod N (1999) Generalizing and extending the eigenshape method of shape space visualization and analysis. *Paleobiology* 25(1):107–138.
15. Piazza P, et al. (2010) *Arabidopsis thaliana* leaf form evolved via loss of KNOX expression in leaves in association with a selective sweep. *Curr Biol* 20(24):2223–2228.
16. Sicard A, et al. (2014) Repeated evolutionary changes of leaf morphology caused by mutations to a homeobox gene. *Curr Biol* 24(16):1880–1886.
17. Hasson A, et al. (2011) Evolution and diverse roles of the *CUP-SHAPED COTYLEDON* genes in Arabidopsis leaf development. *Plant Cell* 23(1):54–68.
18. Todesco M, et al. (2012) Natural variation in biogenesis efficiency of individual *Arabidopsis thaliana* microRNAs. *Curr Biol* 22(2):166–170.
19. deVicente MC, Tanksley SD (1993) QTL analysis of transgressive segregation in an interspecific tomato cross. *Genetics* 134(2):585–596.
20. Alonso-Blanco C, Koornneef M, Ooijen JWv (2006) QTL analysis. Arabidopsis Protocols, Methods in Molecular Biology, eds Salinas J, Sanchez-Serrano JJ (Humana, Totowa, NJ), pp 79–99.
21. Tuinstra MR, Ejeta G, Goldsbrough PB (1997) Heterogeneous inbred family (HIF) analysis: A method for developing near-isogenic lines that differ at quantitative trait loci. *Theor Appl Genet* 95(5-6):1005–1011.
22. Andrés F, Coupland G (2012) The genetic basis of flowering responses to seasonal cues. *Nat Rev Genet* 13(9):627–639.
23. Lempe J, et al. (2005) Diversity of flowering responses in wild *Arabidopsis thaliana* strains. *PLoS Genet* 1(1):109–118.
24. Michaels SD, Amasino RM (1999) *FLOWERING LOCUS C* encodes a novel MADS domain protein that acts as a repressor of flowering. *Plant Cell* 11(5):949–956.
25. Lee I, Bleecker A, Amasino R (1993) Analysis of naturally occurring late flowering in *Arabidopsis thaliana*. *Mol Gen Genet* 237(1-2):171–176.
26. Angel A, Song J, Dean C, Howard M (2011) A Polycomb-based switch underlying quantitative epigenetic memory. *Nature* 476(7358):105–108.
27. Coustham V, et al. (2012) Quantitative modulation of polycomb silencing underlies natural variation in vernalization. *Science* 337(6094):584–587.
28. Finnegan EJ, Dennis ES (2007) Vernalization-induced trimethylation of histone H3 lysine 27 at *FLC* is not maintained in mitotically quiescent cells. *Curr Biol* 17(22): 1978–1983.
29. Heo JB, Sung S (2011) Vernalization-mediated epigenetic silencing by a long intronic noncoding RNA. *Science* 331(6013):76–79.
30. Li P, et al. (2014) Multiple *FLC* haplotypes defined by independent *cis*-regulatory variation underpin life history diversity in *Arabidopsis thaliana*. *Genes Dev* 28(15): 1635–1640.
31. Sheldon CC, Conn AB, Dennis ES, Peacock WJ (2002) Different regulatory regions are required for the vernalization-induced repression of *FLOWERING LOCUS C* and for the epigenetic maintenance of repression. *Plant Cell* 14(10):2527–2537.
32. Sung S, et al. (2006) Epigenetic maintenance of the vernalized state in *Arabidopsis thaliana* requires LIKE HETEROCHROMATIN PROTEIN 1. *Nat Genet* 38(6):706–710.
33. Gould SJ (1977) *Ontogeny and Phylogeny* (Harvard Univ Press, Cambridge, MA), p 522.
34. Hudson CJ, et al. (2014) Genetic control of heterochrony in Eucalyptus globulus. Genes Genomes Genet 4(7):1235–1245.
35. Deng W, et al. (2011) FLOWERING LOCUS C (FLC) regulates development pathways throughout the life cycle of *Arabidopsis*. *Proc Natl Acad Sci USA* 108(16):6680–6685.
36. Willmann MR, Poethig RS (2011) The effect of the floral repressor *FLC* on the timing and progression of vegetative phase change in Arabidopsis. *Development* 138(4): 677–685.
37. Poethig RS (2013) Vegetative phase change and shoot maturation in plants. Current Topics in Developmental Biology (Academic, New York), Vol 105, pp 125–152.
38. Schwarz S, Grande AV, Bujdoso N, Saedler H, Huijser P (2008) The microRNA regulated SBP-box genes *SPL9* and *SPL15* control shoot maturation in Arabidopsis. *Plant Mol Biol* 67(1-2):183–195.
39. Wang JW, et al. (2011) miRNA control of vegetative phase change in trees. *PLoS Genet* 7(2):e1002012.
40. Telfer A, Bollman KM, Poethig RS (1997) Phase change and the regulation of trichome distribution in *Arabidopsis thaliana*. *Development* 124(3):645–654.
41. Searle I, et al. (2006) The transcription factor FLC confers a flowering response to vernalization by repressing meristem competence and systemic signaling in Arabidopsis. *Genes Dev* 20(7):898–912.
42. Turck F, Fornara F, Coupland G (2008) Regulation and identity of florigen: FLOWERING LOCUS T moves center stage. *Annu Rev Plant Biol* 59(1):573–594.
43. Usami T, Horiguchi G, Yano S, Tsukaya H (2009) The more and smaller cells mutants of *Arabidopsis thaliana* identify novel roles for *SQUAMOSA PROMOTER BINDING PROTEIN-LIKE* genes in the control of heteroblasty. *Development* 136(6):955–964.
44. Alonso-Blanco C, Blankestijn-de Vries H, Hanhart CJ, Koornneef M (1999) Natural allelic variation at seed size loci in relation to other life history traits of *Arabidopsis thaliana*. *Proc Natl Acad Sci USA* 96(8):4710–4717.
45. Li Y, Huang Y, Bergelson J, Nordborg M, Borevitz JO (2010) Association mapping of local climate-sensitive quantitative trait loci in *Arabidopsis thaliana*. *Proc Natl Acad Sci USA* 107(49):21199–21204.
46. Taiz L, Zeiger E (2010) Translocation in the phloem. *Plant Physiology* (Sinauer Associates Inc., Sunderland, MA), 5th Ed.
47. Guo Y-L, Todesco M, Hagmann J, Das S, Weigel D (2012) Independent *FLC* mutations as causes of flowering-time variation in *Arabidopsis thaliana* and *Capsella rubella*. *Genetics* 192(2):729–739.
48. Méndez-Vigo B, de Andrés MT, Ramiro M, Martínez-Zapater JM, Alonso-Blanco C (2010) Temporal analysis of natural variation for the rate of leaf production and its relationship with flowering initiation in *Arabidopsis thaliana*. *J Exp Bot* 61(6): 1611–1623.
49. Tadege M, et al. (2001) Control of flowering time by *FLC* orthologues in *Brassica napus*. *Plant J* 28(5):545–553.
50. Wang R, et al. (2009) *PEP1* regulates perennial flowering in *Arabis alpina*. *Nature* 459(7245):423–427.
51. Méndez-Vigo B, Picó FX, Ramiro M, Martínez-Zapater JM, Alonso-Blanco C (2011) Altitudinal and climatic adaptation is mediated by flowering traits and *FRI*, *FLC*, and *PHYC* genes in Arabidopsis. *Plant Physiol* 157(4):1942–1955.
52. Martin A, Orgogozo V (2013) The Loci of repeated evolution: A catalog of genetic hotspots of phenotypic variation. *Evolution* 67(5):1235–1250.
53. Stern DL, Orgogozo V (2009) Is genetic evolution predictable? *Science* 323(5915): 746–751.
54. Ashby E (1948) Studies in the morphogenesis of leaves. *New Phytol* 47(2):153–176.
55. Stephens SG (1944) The genetic organization of leaf-shape development in the genus *Gossypium*. *J Genet* 46(1):28–51.
56. Costa MMR, et al. (2012) The genetic basis for natural variation in heteroblasty in *Antirrhinum*. *New Phytol* 196(4):1251–1259.
57. Shalit A, et al. (2009) The flowering hormone florigen functions as a general systemic regulator of growth and termination. *Proc Natl Acad Sci USA* 106(20):8392–8397.
58. Broman KW, Wu H, Sen S, Churchill GA (2003) R/qtl: QTL mapping in experimental crosses. *Bioinformatics* 19(7):889–890.
59. International VSN (2013) *GenStat for Windows* (VSN International, Hemel Hempstead, U.K.), 16th Ed.
60. Zahn CT, Roskies RZ (1972) Fourier descriptors for plane closed curves. *IEEE Trans Comput* 21(3):269–281.